Reverse Thermal Gelling PEG−PTMC Diblock Copolymer Aqueous Solution

So Young Kim,[†] Hyun Jeong Kim,[†] Kyung Eun Lee,[‡] Sung Sik Han,[‡] Youn Soo Sohn,[†] and Byeongmoon Jeong*[,†]

Department of Chemistry, Division of Nano Science, Ewha Womans University, Daehyun-Dong, Seodaemun-Ku, Seoul 120-750, Korea, and Division of Life Science, College of Life Science and Biotechnology, Korea University, Anam-Dong, Seongbuk-Ku, Seoul 136-701, Korea

Received January 24, 2007; Revised Manuscript Received April 27, 2007

ABSTRACT: In the search for a new thermogelling biomaterial, we are reporting poly(ethylene glycol)−poly(trimethylene carbonate) (PEG−PTMC) diblock copolymers. The PEG−PTMC (550−2750) diblock copolymer aqueous solutions (>25 wt %) underwent sol-to-gel-to-syneresis (macroscopic phase separation between the polymer and water) transition as the temperature increased. The sol-to-gel transition temperature could be controlled in a range of 20−75 °C by varying polymer concentration in water, molecular weight, and composition of the polymer. ^{13}C NMR spectra, a transmission electron microscopic image, and dynamic light scattering suggest that the micellar aggregation through the dehydration of PEG is involved in the sol-to-gel transition. The in-situ gel formation was confirmed by subcutaneous injection of the polymer aqueous solution (30 wt %, 0.5 mL) into rats. Because of the diffusion of the polymer with a low molecular weight out of the gel, mass loss of 15 wt % was observed over 20 days in in-vivo study. On the other hand, the polymer is so stable in phosphate buffer saline that any changes in molecular weight, pH, and gel mass were not observed over the same period of time in in-vitro study.

Introduction

As a degradable biomaterial, aliphatic polyesters such as homo- and copolymers of glycolide, L- or DL-lactide, caprolactone, and butyrolactone have been extensively studied for suture, drug delivery, tissue engineering, and artificial organ applications.[1−3] As another class of biomaterial, aliphatic polycarbonate has been drawing attention.[4−6] In particular, poly(trimethylene carbonate) (PTMC) showed some attractive characteristics as a biomaterial such as facile preparation by cationic polymerization, biocompatibility, and mechanical softness.[7−9]

Reverse thermal gelling materials are suggested to be very promising implantable biomaterials for drug delivery and tissue engineering applications because (1) a surgical procedure is not needed to make an implant, (2) sterilization is simple by microfiltration in a sol state, and (3) organic solvent is not used during the fabrication of the implant.[10,11] A mild change in temperature induces the transition from a low viscous sol to a semisolid gel. Therefore, sensitive therapeutic agents including protein drugs or cells can be incorporated in a sol state, followed by injection into a target site can make the hydrogel depot system due to the heat induced sol-to-gel transition.[12,13] To show a temperature-induced sol-to-gel transition in water, the polymer should have a delicate balance of hydrophobicity and hydrophilicity.[14,15] Poly(ethylene glycol) (PEG) has typically been used for the hydrophilic part due to its proven biocompatibility.[16] Poly(lactic acid-*co*-glycolic acid), polycaprolactone, polyphosphazene, poly(propylene fumarate), chitosan, and their modified structures have been used for the biodegradable hydrophobic part.[17−24] Poly(lactic acid)/poly(dimethyl-β-malic acid-*co*-β-butyrolactone) consisting of purely biodegradable blocks was also reported as a reverse polymer, where the poly(dimethyl-β-malic acid-*co*-β-butyrolactone) block acts as a hydrophilic part.[25]

In this research, we prepared a series of poly(ethylene glycol)−poly(trimethylene carbonate) (PEG−PTMC) diblock copolymers.[26,27] The molecular weights of PEG (hydrophilic block) and PTMC (hydrophobic block) were controlled to prepare a polymer showing reverse thermal gelation. Molecular aggregation behavior in water, the structure−property relationship of sol−gel transition, and in-vitro/in-vivo degradation behavior of the PEG−PTMC diblock polymer were investigated. The characteristics of PEG−PTMC as an injectable material were compared with the previous reverse thermal gelling polymer systems.

Experimental Section

Materials. Trimethylene carbonate (Aldrich), stannous octoate (Aldrich), monomethoxy poly(ethylene glycol) (MW = 550 (Fluka), 750 (Aldrich), and 1100 (Fluka)), 1,6-diphenyl-1,3,5-hexatriene (Aldrich), and 2-anilinonaphthalene (TCI) were used as received. Toluene (Aldrich) was dried over sodium before use.

Synthesis. PEG−PTMC diblock copolymers were prepared by the ring-opening polymerization of trimethylene carbonate on the monomethoxypoly(ethylene glycol). Stannous octoate was used as a catalyst. For example, to synthesize the PEG−PTMC diblock copolymer (550−2750) (PI in Table 1), the monomethoxypoly(ethylene glycol) (4.4 g, 8.0 mmol, MW = 550) was dissolved in anhydrous toluene (80 mL), and the solvent was distilled off to a final volume of 30 mL to remove the residual water adsorbed to the polymer. Trimethylene carbonate (14.4 g, 141 mmol) and stannous octoate (25 μL, 0.062 mmol) were added to the reaction mixture and stirred at 120 °C for 24 h. The product was isolated by precipitation into diethyl ether. The polymer was dissolved in methylene chloride and fractionally precipitated by slowly adding diethyl ether. Two times the fractional precipitation separated the diblock copolymer with a final yield of 65%. The residual solvent was removed under vacuum. Other PEG−PTMC diblock copolymers in Table 1 were similarly synthesized.

Gel Permeation Chromatography. The gel permeation chromatography system (Waters 515) with a refractive index detector

* Corresponding author: e-mail bjeong@ewha.ac.kr, Fax 82-2-3277-3411.
[†] Ewha Womans University.
[‡] Korea University.

10.1021/ma070190z CCC: $37.00
Published on Web 06/21/2007

Table 1. List of PEG−PTMC Diblock Copolymers Studied

	PEG−PTMC[a]	M_n[a]	EG/TMC[a]	M_n[b]	M_w/M_n[b]
PI	$(EG)_{12.5}-(TMC)_{27.0}$	550−2750	0.46	4700	1.4
PII	$(EG)_{12.5}-(TMC)_{29.4}$	550−3000	0.42	5600	1.5
PIII	$(EG)_{17.0}-(TMC)_{29.4}$	750−3000	0.58	6500	1.4
PIV	$(EG)_{17.0}-(TMC)_{41.7}$	750−4250	0.40	7700	1.5
PV	$(EG)_{25.0}-(TMC)_{29.4}$	1100−3000	0.84	8100	1.4
PVI	$(EG)_{25.0}-(TMC)_{59.8}$	1100−6100	0.42	12000	1.5

[a] Determined by ^{1}H NMR in $CDCl_3$ based on ethylene glycol (EG) unit (4H, 3.6 ppm) and trimethylene carbonate (TMC) unit (4H, 4.3 ppm) of the polymers. [b] Determined by GPC. In the GPC, tetrahydrofuran was used as an eluting solvent, and polystyrenes in a molecular weight range of 1000−20 000 were used as the molecular weight standards.

(Waters 410) was used to obtain molecular weight and molecular weight distributions of polymers. Tetrahydrofuran was used as an eluting solvent. The polystyrenes in a molecular weight range of 1000−20 000 Da were used as the molecular weight standards. Styragel HMW 6E and HR 4E columns (Waters) were used in series.

NMR Study. A 500 MHz NMR spectrometer (Varian) was used for ^{1}H NMR (in $CDCl_3$) to study composition of the polymer and ^{13}C NMR (in D_2O) to see the spectral change of the PEG−PTMC diblock copolymer as a function of temperature. The solution temperature was equilibrated for 20 min before the measurement.

Sol−Gel Transition. The sol−gel transition temperature was determined by the test tube inverting method and dynamic mechanical analysis. For the test tube inverting method, the 4 mL vials (diameter 1.1 cm) containing 0.5 mL of PEG−PTMC diblock copolymer solutions were immersed in a water bath at 4 °C for 30 min. The transition temperatures were determined by a flow (sol)−no flow (gel) criterion when the vial was inverted with a temperature increment of 1 °C per step.[28,29] The syneresis temperature was determined by the visual observation of the macroscopic phase separation between the polymer and water. Each data point is an average of three measurements.

The sol-to-gel transition of the polymer aqueous solution was also investigated by dynamic rheometry (Thermo Haake, rheometer RS 1).[30,31] The aqueous polymer solution (PI; 30 wt %) was placed between parallel plates of 25 mm diameter and a gap of 0.5 mm. The data were collected under a controlled stress (4.0 dyn/cm^2) and a frequency of 1.0 rad/s. The heating and cooling rates were 0.2 °C/min. The shear rate dependence of the viscosity was performed for PEG−PTMC (PI) aqueous solution (30 wt %) at 20 °C (sol), 28 °C (sol−gel transition temperature), and 31 °C (gel).

Cryo-Transmission Electron Microscopy. To see the assembled structure of the polymer in water, the aqueous polymer solution (PI; 0.05 or 30 wt %) was coated on a carbon grid and blotted by the filter paper. The sample was rapidly frozen onto liquid ethane (−170 °C). The frozen image of the polymer was obtained using a cryo-transmission electron microscope (Tecnai 12, Philips) with an accelerating voltage of 120 kV.

Critical Aggregation Concentration. Critical aggregation concentration was determined by the fluorescence spectroscopy at room temperature (20 °C). 2-Anilinonaphthalene solution in methanol (30 μL at 0.01 mM) was injected into an aqueous solution (3.0 mL) in a polymer (PI) concentration range of 1.0×10^{-6}−1.0×10^{-1} wt %. The excitation wavelength was 309 nm. The fluorescence spectra of these solutions were recorded from 350 to 600 nm. The band position (λ_{max}) was plotted against the polymer concentration, and the crossing point of the two extrapolated straight lines was defined as the critical aggregation concentration of the polymer in water.[32,33]

Dynamic Light Scattering. The apparent size of a polymer aggregate in water was studied by a dynamic light scattering (DLS) instrument (ALV 5000-60x0) as a function of temperature at 0.05 and 2.0 wt %. A YAG DPSS-200 laser (Langen, Germany) operating at 532 nm was used as a light source. Measurements of scattered light were made at an angle of 90° to the incident beam. The results of DLS were analyzed by the regularized CONTIN method. The decay rate distributions were transformed to an apparent diffusion coefficient (D). From the diffusion coefficient, the apparent hydrodynamic size of a polymer aggregate can be obtained by the Stokes−Einstein equation.

In-Vitro Degradation. Aqueous solutions (0.5 mL) of PEG−PTMC (PI) (30 wt %) was kept at 37 °C for 2 min to form a gel. 3.0 mL of phosphate buffer saline (pH = 7.4, 37 °C) was added to the gel. The medium (3.0 mL) was replaced everyday. In addition, to investigate the storage stability of the PEG−PTMC (PI in Table 1) at room temperature, the aqueous polymer solution (0.5 mL, 30 wt %) was kept at 20 °C for 30, 60, and 90 days. For both cases, the phosphate buffer saline was removed by the freeze-drying method at a given time interval. The polymer was redissolved in tetrahydrofuran for gel permeation chromatography (Waters 515 with a refractive index detector). Polystyrenes were used as the molecular weight standards. Tetrahydrofuran was used as an eluting solvent, and the flow rate was 1.0 mL/min.

In-Vivo Gel Formation and Degradation. 0.5 mL of an aqueous polymer (PI) solution (30 wt %) at 20 °C was injected through a 21 gauge syringe needle into the subcutaneous layer of the rat. The rat was sacrificed at a given time interval, and photos around the implanted site were taken. The remaining gel was freeze-dried, and the molecular weight of the polymer was investigated. The experimental protocol was followed by guidelines set forth in the National Institutes of Health Guide for the Care and Use of Laboratory Animals.

Results and Discussion

The PEG−PTMC diblock copolymer was synthesized by the ring-opening polymerization of trimethylene carbonate onto the monomethoxy-PEG in the presence of stannous octoate as a catalyst. The ratio of ^{1}H NMR peak area at 4.3 ppm ($A_{4.3}$) to 3.6 ($A_{3.6}$) ppm gives the number-average molecular weight of the PEG−PTMC diblock copolymer by the following equations (Supporting Information, Figure S1-a). For $CH_3O-(CH_2CH_2O)_n-(COOCH_2CH_2CH_2O)_mH$

$$m/n = A_{4.3}/A_{3.6}$$

$$M_n(\text{PEG}) = 32 + 44n$$

$$M_n(\text{PEG-PTMC}) = 32 + 44n + 102m$$

n values are 12.5, 17.0, and 25.0 for PEG 550, PEG 750, and PEG1100, respectively.

The polymers studied in this research are listed in Table 1. ^{1}H NMR peaks at 3.6 ppm (CH_2CH_2O) and 4.3 ppm ($COOCH_2$-CH_2CH_2O) (Figure S1-a),[34] FTIR peaks (Figure S1-b) at 1747 cm^{-1} (O−*CO*−O carbonate stretching) and 1100−1200 cm^{-1} (*CO* ether stretching),[35] and gel permeation chromatograms (Figure S1-c) of PEG (MW ∼ 550 Da) (retention time = 19.5 min) and PEG−PTMC (PI) (retention time = 16.5 min) support the formation of the PEG−PTMC diblock copolymer (Supporting Information, Figure S1).

The PEG−PTMC diblock copolymer aqueous solution underwent sol (slightly bluish)-to-gel (turbid) transition as the temperature increased. Further increase in temperature resulted in a macroscopic phase separation between the polymer and water (syneresis). For example, the PEG−PTMC (550−2750; PI) aqueous solution (30 wt %) underwent sol-to-gel transition at 28 °C and gel-to-syneresis transition at 38 °C. The typical phase diagram of PEM−PTMC (PI) and photos of the sol (at 20 °C) and gel (at 35 °C) phases are shown (Figure 1a,b). During the sol-to-gel transition, an abrupt increase in the modulus from 1.0 to 10 000 mPa was observed (Figure 1c).[30,36] The gel modulus of PEG−PTMC (PI) (∼10 Pa) was low enough to be injected through a 21 gauge syringe needle as a gel state. The PLGA/PEG and PEG/PCL were reported to have about 100−

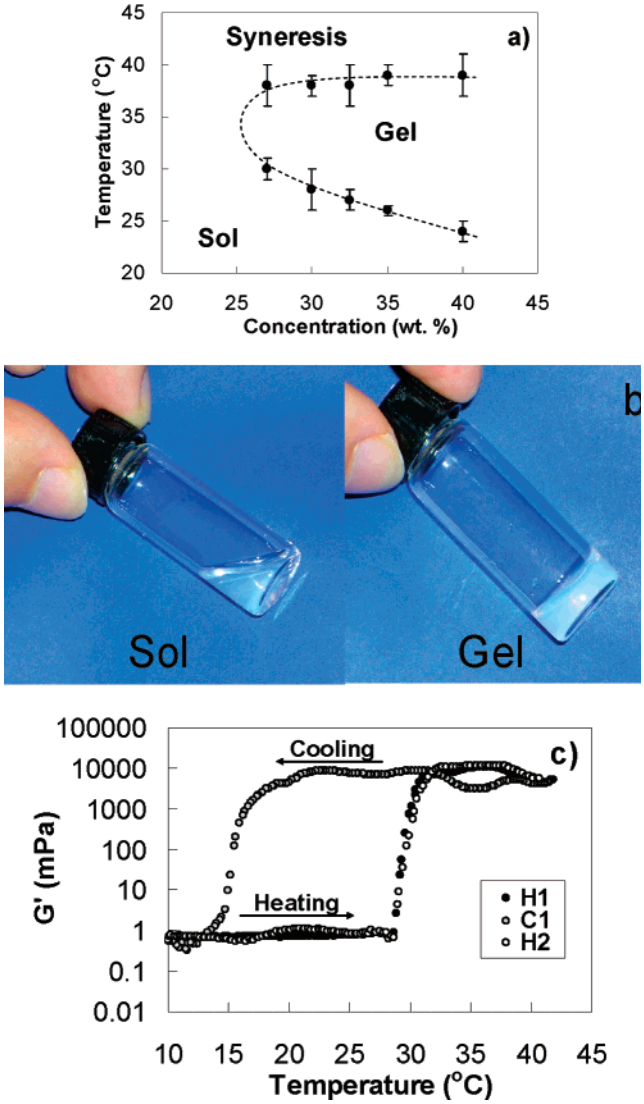

Figure 1. (a) Phase diagram of the PEG−PTMC diblock copolymer (PI) in water. The transition temperature was measured by the test tube inverting method. Each data point is an average of three measurements. (b) Photo showing the sol (at 20 °C) and the gel (at 35 °C) states of the PEG−PTMC diblock copolymer (PI) aqueous solution (30 wt %). (c) Changes in the modulus of the PEG−PTMC diblock copolymer (PI) aqueous solutions (30 wt %) as a function of temperature during the heating → cooling → heating cycle. H1, C1, and H2 indicate the first heating, the first cooling, and the second heating cycle, respectively.

1000 Pa in the gel state.[30,36] When the temperature decreased, the PEG−PTMC gel reversibly turned into a sol. The dynamic mechanical analysis showed a hysteresis loop because the absorption of the water in a gel state (cooling) is kinetically slower than the sol-to-gel-to syneresis transition process (heating) of a dissolved polymer. However, once PEG−PTMC formed a sol at low temperature, the sol-to-gel transition in the second heating cycle occurred at the same temperature with the first heating cycle (Figure 1c), suggesting the reversibility of the sol−gel transition. Even when the gel prepared from aqueous polymer solution (30 wt %) was kept at 37 °C for 20 days, the same sol-to-gel transition at 28 °C was observed. This fact suggests the reversibility of the sol−gel transition and nondegradability of the PEG−PTMC in water as will be discussed later.

The viscosity of PI (30 wt % in water) at 20 °C (sol), 28 °C (sol-to-gel transition temperature), and 35 °C (gel) was compared as a function of shear rate. The viscosity of the gel phase was 1000−10 000 times larger than that of the sol phase in a shear

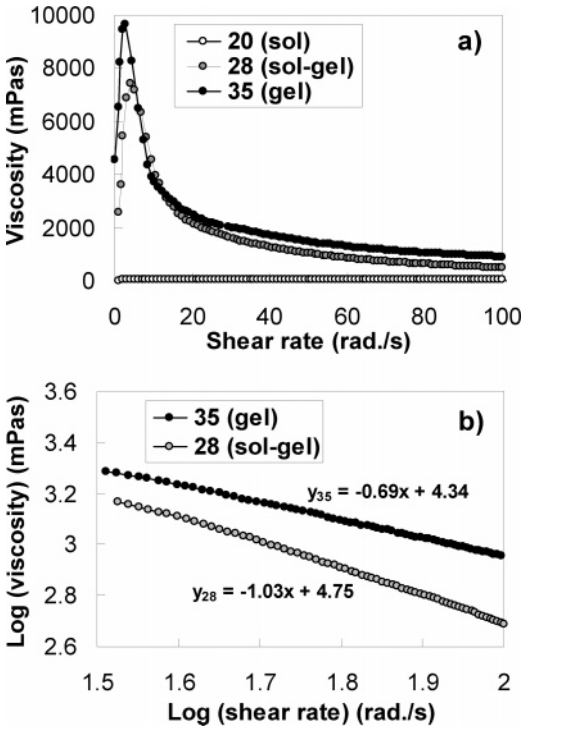

Figure 2. (a) Viscosity of the PEG−PTMC diblock copolymer (PI) aqueous solution (30 wt %) as a function of shear rate in sol state (at 20 °C), sol−gel transition temperature (28 °C), and gel state (at 35 °C). (b) The power law equations are shown for the shear-thinning region where the shear rate is greater than 30.0 rad/s.

rate range of 1.0−100 rad/s (Figure 2a). The viscosity of sol is nearly independent of the shear rate, indicating that the sol behaves like a Newtonian fluid. However, the viscosity was maximal at about 3.0 rad/s at the sol-to-gel transition temperature (28 °C) and in the gel state (35 °C). This behavior can be explained as follows. In a low shear rate region, the gel with physical junctions resists against the shear stress. Therefore, the viscosity increases as the shear rate increases. However, when the shear rate is large enough (>4.0 rad/s) to break the physical junctions of the aggregates, the viscosity decreases as the shear rate increases. Such a maximum curve was also observed for physical gel of colloidal dispersions of stearyl-coated silica particles.[37] The shear-thinning region was plotted to obtain the power law exponent (a) (Figure 2b).

$$\eta = K(\mathrm{d}\gamma/\mathrm{d}t)^{-a}$$

Therefore, $\log \eta = -a \log(\mathrm{d}\gamma/\mathrm{d}t) + \log K$, where K is the proportionality constant and $\mathrm{d}\gamma/\mathrm{d}t$ is the shear rate. The power law exponents in the shear thinning region were simulated to be 1.03 at 28 °C (sol−gel transition) and 0.69 at 35 °C (gel). Because the system has tighter physical junctions in the gel state than the sol−gel transition state, the viscosity decayed more slowly in the gel state than the sol−gel transition state.

To gain insight into the phase transition mechanism at the molecular level, the ^{13}C NMR spectrum of the polymer (30 wt %) was studied as a function of temperature in deuterated water (Figure 3). In the sol state (20 °C), the hydrophilic PEG peak at 69−70 ppm was sharp whereas the hydrophobic PTMC peak at 63−65 ppm was collapsed. The sharpness of a peak in ^{13}C NMR reflects a highly dynamic state of the block.[19,22,30,38] When the PEG−PTMC forms a core−shell structure, as would be proven in the TEM image at 30 wt %, the molecular motion of the core block (PTMC) of a micelle is restricted, where the shell block (PEG) is in a highly dynamic state. Therefore, the

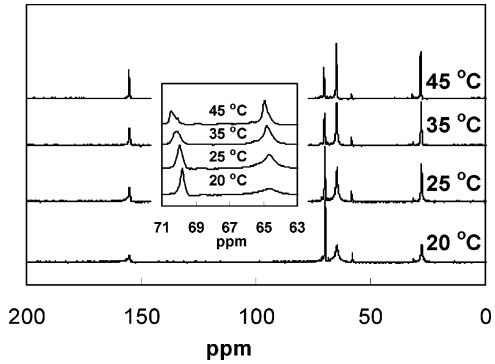

Figure 3. ^{13}C NMR spectra of PEG−PTMC (PI) aqueous solutions (30 wt %) in D_2O as a function of temperature. The spectra at 20 °C (sol), 25 °C (just below sol-to-gel transition), 35 °C (gel), and 45 °C (above syneresis) were compared.

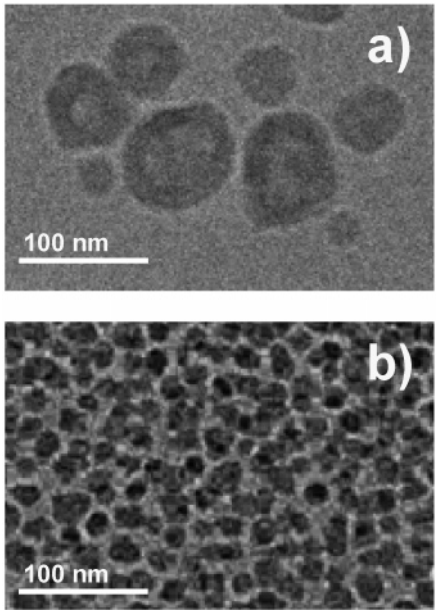

Figure 4. Cryo-transmission electron microscopic image of the polymer (PI) aqueous solutions at 20 °C: (a) 0.05 and (b) 30.0 wt %. The scale bar is 100 nm.

PTMC peak is collapsed, and the PEG peak is sharp in the NMR at 20 °C. When the micelles experience a transition from sol-to-gel state, the molecular motion of PTMC increases by thermal energy, whereas the PEG are dehydrated and entangled to form a gel; thus, the molecular motion of the PEG is rather restricted as the temperature increases. Because of the dehydration of PEG, a decrease (∼30%) in the hydrodynamic radius of monomethoxy PEG (MW∼ 550) in water was reported when the temperature increased from 20 to 45 °C.[39] The extent of dehydration was more pronounced when the PEG is covalently bonded to a hydrophobic moiety. A further increase in temperature makes the gel-to-syneresis transition. During this transition, further dehydration of the PEG occurs and the molecular motion of PEG is more restricted, resulting in the collapsed PEG peak in the NMR spectra, whereas the PTMC molecular motion is further increased due to the increased thermal energy.

To see the nature of the polymer aggregation in water, cryo-TEM images of the polymer solutions at low (0.05 wt %) and high (30.0 wt %) concentrations at 20 °C were investigated (Figure 4). The cryo-TEM image showed coexistence of micelles and vesicles at low concentration. Vesicle formation might come from the relative large molecular weight of hydrophobic block compared with hydrophilic blocks. The molecular weight ratio of hydrophobic block to hydrophilic block showing reverse thermal gelation was 0.9−2.5 for PEG/PLGA and PEG/PCL systems.[17,18] The molecular weight ratio of PTMC to PEG of current PEG−PTMC (550−2740) is 5.0. This ratio is much larger than previous reverse thermal gelling polymers that showed only micelles at low concentrations. As the size of the hydrophobic part increases, the surfactants tend to from a vesicle with a bilayer structure.[40] The coexistence of micelles and vesicles at low polymer concentration in water was also reported for poly(2-hydroxyethyl aspartamide)-*g*-poly(lactide).[41] At high concentration (30 wt %), spheres with an average size of 25 nm were observed. Such a decrease in the aggregate size with increasing polymer concentration coincided with the results of light scattering as will be discussed in the section on light scattering.

The core−shell type aggregation was confirmed by fluorescence spectra of 2-anilinonaphthalene as a function of PEG−PTMC concentration in water (Figure 4a). The emission wavelength of 2-anilinonaphthalene is sensitive to the solvent polarity. In a polar (hydrophilic) environment, the λ_{max} is observed at about 445 nm; however, the λ_{max} shifted to 410 nm in a nonpolar hydrophobic environment. At a low polymer concentration, the 2-anilinonaphthalene is exposed to a polar aqueous environment. As the polymer concentration increased, the PEG−PTMC diblock copolymers would aggregate to form a core−shell type structure in water, and the hydrophobic dye (2-anilinonaphthalene) would be partitioned into the hydrophobic core. λ_{max} was plotted against the polymer concentration to obtain the critical concentration for the polymer aggregation.[32,33] The crossing point of two extrapolated lines was defined as the critical aggregation concentration of the polymer in water, which was about 5×10^{-5} wt % (Figure 4b). This is quite small compared with previous thermogelling polymers of PEG/PLGA, PEG/PCL, etc., which was about 10^{-2} wt %.[18,42] This behavior is related to the large fraction of hydrophobic block (PTMC) in PEG−PTMC (550−2750) compared with PEG/PLGA (550/1400) and PEG/PCL (550/1000) which shows a reverse thermal gelling property at about 30 °C.

The apparent size of a polymer aggregate was investigated as a function of temperature by dynamic light scattering. As the temperature increased from 20 to 35 °C at 0.05 wt %, the size decreased from 80 to 60 nm and the size distribution of the polymer aggregates decreased (Figure 6a). The shrinkage of the polymer aggregate as the temperature increased might be correlated to the partial dehydration of the PEG, as was discussed in the previous section on ^{13}C NMR spectra. At 20 °C, the polymer aggregate size was smaller at 2.0 wt % (45 nm) than 0.05 wt % (80 nm). As the temperature increased, however, the most probable aggregate size increased from 45 nm (20 °C) to 190 nm (35 °C) and to 295 nm (45) °C (Figure 6b). This observation suggests that extensive micellar aggregation might occur during the sol-to-gel transition.

The effect of PEG molecular weight in the PEG−PTMC block copolymer on the sol−gel phase diagrams is shown in Figure 7a. The sol-to-gel transition temperature increased from 25−35 to 53−54 °C, and the gel window decreased as the PEG molecular weight increased from 550 to 750 Da at a fixed molecular weight of PTMC (∼3000 Da). When the PEG molecular weight increased to 1000 Da, PEG−PTMC (1000−3000; PV), the sol-to-gel transition was not observed in a temperature range of 0−100 °C. This observation suggests that the hydrophobic interactions are a major driving force of sol-

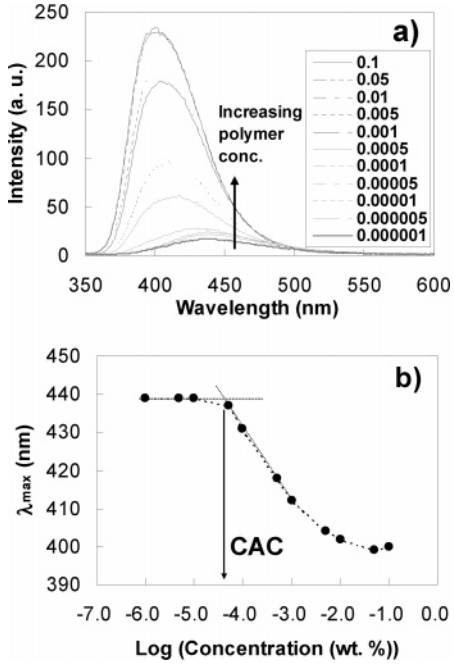

Figure 5. (a) Fluorescence spectra of 2-anilinonaphthalene as a function of polymer (PI) concentration in water at 20 °C. The legends are polymer concentration (wt %) in water. The dye concentration was fixed at 1.0×10^{-5} M. (b) Critical aggregate concentration of the polymer was defined by a crossing point of the two extrapolated lines.

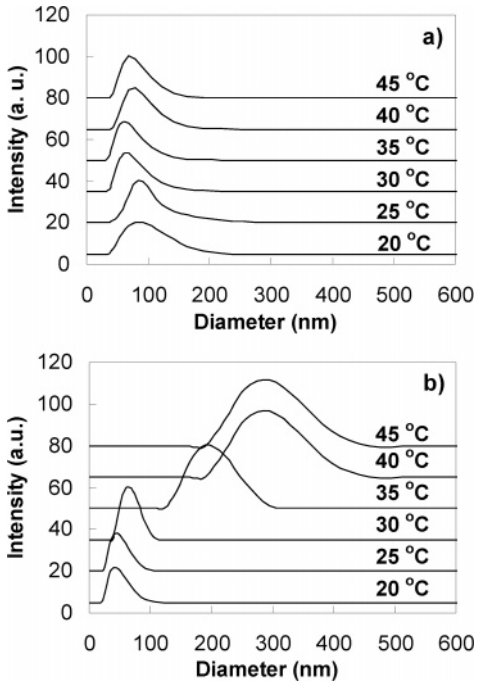

Figure 6. Apparent aggregate size of PEG−PTMC diblock copolymer (PI) in water as a function of temperature at 0.05 wt % (a) and at 2.0 wt % (b).

to-gel transition of the PEG−PTMC aqueous solution. As the PEG length increased, the aggregation is blocked due to the highly dynamic motion of PEG in water.[43]

At a fixed ratio of PTMC/PEG (by molecular weight) of 5.5, the sol-to-gel transition temperature increased as both the PEG and PTMC molecular weight increased (Figure 7b). Therefore, the composition as well as the block length is critical in designing a polymer showing sol-to-gel transition in a physiologically important temperature range of 30−45 °C.

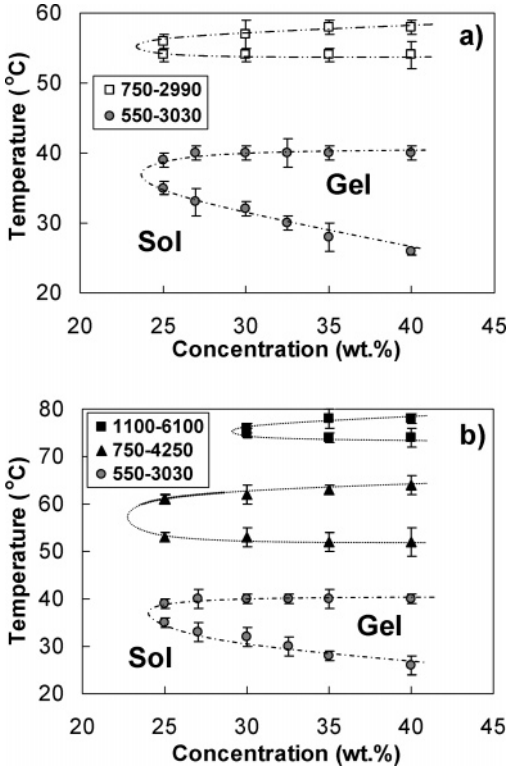

Figure 7. Control of phase diagram of PEG−PTMC diblock copolymer aqueous solutions measured by the test tube inverting method: (a) effect of PEG molecular weight at a fixed PTMC block length; (b) effect of the block length at a fixed composition (PTMC/PEG = 5.5). The legends are the molecular weights of each block in the PEG−PTMC. Each data point is an average of three measurements.

On the basis of the ^{13}C NMR spectra, transmission electron microscopic images, fluorescence study, dynamic light scattering, and structure−property relationship, a sol-to-gel transition mechanism of PEG-PTMC aqueous solution could be suggested as follows. The diblock copolymers consisting of hydrophilic PEG and hydrophobic PTMC blocks form micelles in water at high concentration (TEM image at 30 wt %). As the temperature increases, micelles aggregate to form a continuous network, resulting in the gel formation. As the PEG block length increased from 550 to 1100, micelle conformation changes from a crew-cut type to a more stable hairy type;[44] therefore, more severe conditions are needed for phase separation to occur, resulting in the high sol-to-gel transition temperature. The fact that gel is soft for a highly concentrated system suggests that the coalesced micelles are merely in contact without significant mutual interactions that would increase a resistance to deformation.

To test the biomedical applicability, 0.5 mL of the PEG−PTMC (PI) aqueous solution (30 wt %) was subcutaneously injected into the rats. The in-situ gel formation was confirmed by investigating the gel in the injection site 1 day after the injection. The polymer slowly disintegrated over 20 days in rats. Photos taken 1, 3, 10, and 20 days after the injection of the polymer aqueous solutions are shown in Figure S2 (Supporting Information). The remaining gel in the rat (in-vivo) was collected, and the change in molecular weight was monitored (Figure 8a). Degradation of the polymer hydrogel prepared from the same PEG−PTMC (PI) aqueous solution (0.5 mL, 30 wt %) was compared in the phosphate buffer saline (in-vitro) over the same period (Figure 8b). To mimic the continuous flow of the body fluid in in-vivo conditions, the phosphate buffer saline was replaced every day in the in-vitro experiment. The degrada-

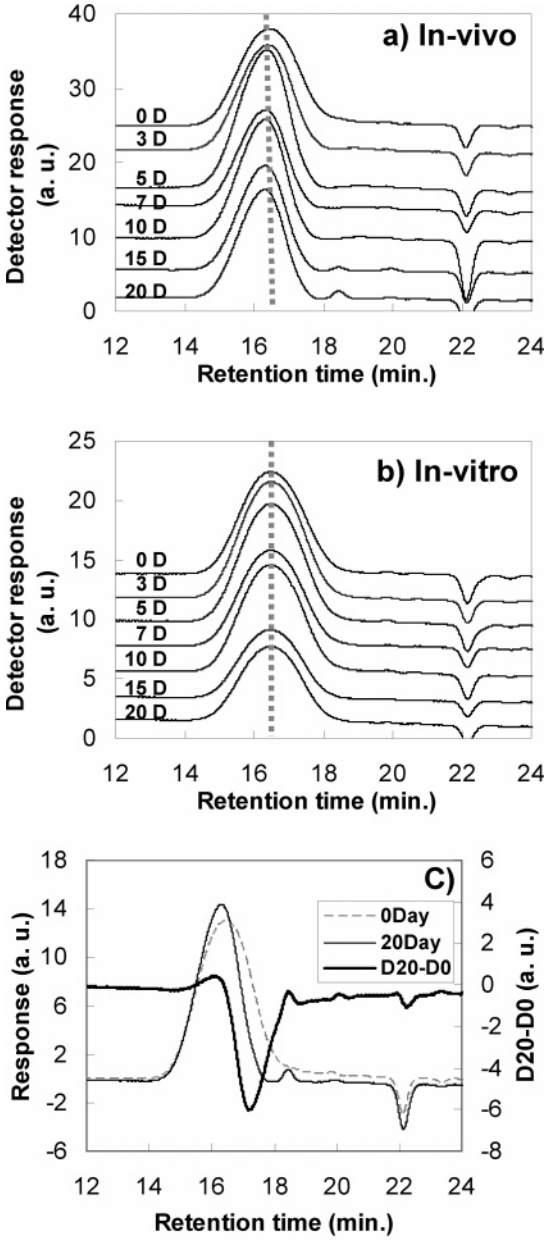

Figure 8. Gel permeation chromatogram of the remaining gel during degradation of the PEG−PTMC. *n*D is the polymer sampled *n* days after starting degradation study. (a) In-vivo study. (b) In-vitro study. (c) Subtracted chromatogram of D0 from D20 of the in-vivo study. The new bands (convex) and eliminated band (concave) are clearly shown.

tion behavior of the PEG−PTMC is quite different from previous reverse thermogelling PEG/PLGA systems. PEG−PTMC showed around 15% mass loss over 20 days in the subcutaneous layer of rats. Gel permeation chromatogram showed an elimination of lower molecular weight fraction that was clearly seen by the subtraction of the 0th day chromatogram from the 20th day chromatogram (Figure 8c). A small fraction of low molecular weight products at 18.4 and 19.9 min, corresponding to 1350 and 500 Da, appeared only in in-vivo samples. On the other hand, the reverse thermogelling PEG/PLGA showed a decrease in molecular weight from 4500 to 3000 Da and 30% mass loss over 1 month in rats.[45] In addition, the PEG−PTMC polymer gel did not undergo any change in mass or molecular weight in phosphate buffer saline in the same period of time, whereas the PEG/PLGA showed that a significant polymer degradation occurred in phosphate buffer saline as well as in in-vivo. In fact, the PEG−PTMC did not undergo any change in mass or molecular weight in 90 days in phosphate buffer saline (Supporting Information, Figure S3). Therefore, we can conclude that PEG−PTMC is quite stable in the in-vitro system (phosphate buffer saline) and slightly degradable and erodable of low molecular weight fraction from the gel in in-vivo.

Conclusions

To conclude, reverse thermal gelling PEG−PTMCs were developed and their physicochemical characteristics in water were studied. PEG−PTMC aqueous solutions (>25 wt %) underwent a sol-to-gel transition as the temperature increased. With further increase in temperature, a macroscopic phase separation between the polymer and water occurred. The sol-to-gel transition temperature could be controlled over 25−75 °C depending on the polymer concentration in water, composition, and molecular weight of the PEG−PTMC block copolymer. The sol behaved like a Newtonian fluid, whereas the gel showed shear thickening at a low shear rate region and shear thinning at a high shear rate region. The cryo-transmission electron microscopic images, dynamic light scattering, and ^{13}C NMR study suggest that micellar aggregation through the dehydration of the PEG seem to be involved in the sol-to-gel transition.

The PEG−PTMC diblock copolymer did not degrade in phosphate buffer saline at room temperature over 90 days. However, the in-situ formed gel in the subcutaneous layer of the rats was partially eroded. By taking such advantages, the PEG−PTMC can be used as an in-situ gel-forming biomaterial for drug delivery and tissue engineering.

Acknowledgment. This work was supported by the SRC program of MOST/KOSEF through the Center for Intelligent Nano-Bio Materials at Ewha Womans University (Grant R11-2005-008-00000-00), Korea Research Foundation (Grant KRF-2004-005-C00090), and Seoul R&BD Program (10816).

Supporting Information Available: ^{1}H NMR and FTIR spectra, gel permeation chromatogram of the PEG−PTMC (PI), photos taken 1, 3, 10, and 20 days after the subcutaneous injection of the PEG−PTMC aqueous solution (30 wt %; 0.5 mL/rat) into the rats, and GPC traces of the PEG−PTMC (550−2750) during storage for 30, 60, and 90 days at room temperature (20 °C) in phosphate buffer saline (30 wt %, 0.5 mL). This material is available free of charge via the Internet at http://pubs.acs.org.

References and Notes

(1) Ueda, H.; Tabata, Y. *Adv. Drug Delivery Rev.* **2003**, *55*, 501−518.
(2) Albertsson, A.-C.; Varma, I. K. *Biomacromolecules* **2003**, *4*, 1466−1486.
(3) Sodergard, A.; Stolt, M. *Prog. Polym. Sci.* **2002**, *27*, 1123−1163.
(4) Zhu, K. J.; Hendren, R. W.; Jensen, K.; Pitt, C. G. *Macromolecules* **1991**, *24*, 1736−1740.
(5) Wang, H.; Dong, J. H.; Qui, K. Y. *J. Polym. Sci., Polym. Chem. Ed.* **1998**, *36*, 695−702.
(6) Kim, C.; Lee, S. C.; Shin, J. H.; Yoon, J. S.; Kwon, I. C.; Jeong, S. Y. *Macromolecules* **2000**, *33*, 7748−7452.
(7) Zhang, Z.; Kuijer, R.; Bulstra, S. K.; Grijpma, D. W.; Feijen, J. *Biomaterials* **2006**, *27*, 1741−1748.
(8) Zhang, Y.; Zhou, R. *Biomaterials* **2005**, *26*, 2089−2094.
(9) Zhangg, Z.; Grijpma, D. W.; Feijen, J. *J. Controlled Release* **2006**, *112*, 57−63.
(10) Packhaeuser, C. B.; Schnieders, J.; Oster, C. G.; Kissel, T. *Eur. J. Pharmacol. Biopharm.* **2004**, *58*, 445−455.
(11) Huang, K; Lee, B. P.; Ingram, D. R.; Messersmith, P. B. *Biomacromolecules* **2002**, *3*, 397−406.
(12) Choi, S.; Baudy, M.; Kim, S. W. *Pharm. Res.* **2004**, *21*,821−831.
(13) Dang, J. M.; Sun, D. D.; Shin-Ya, Y.; Seiber, A. N.; Kostuik, J. P.; Leong, K. W. *Biomaterials* **2006**, *27*, 406−418.

(14) Jeong, B.; Bae, Y. H.; Lee, D. S.; Kim, S. W. *Nature (London)* **1997**, *388*, 860−862.
(15) Jeong, B.; Kim, S. W.; Bae, Y. H. *Adv. Drug Delivery Rev.* **2002**, *54*, 37−51.
(16) Zhu, K. J.; Lin, X.; Yang, S. *J. Appl. Polym. Sci.* **1990**, *39*, 1−9.
(17) Jeong, B.; Bae, Y. H.; Kim, S. W. *Macromolecules* **1999**, *32*, 7064−7069.
(18) Hwang, M. J.; Suh, J. M.; Bae, Y. H.; Kim, S. W.; Jeong, B. *Biomacromolecules* **2005**, *6*, 885−890.
(19) Lee, B. H.; Lee, Y. M.; Sohn, Y. S.; Song, S. C. *Macromolecules* **2002**, *35*, 3876−3879.
(20) Behravesh, E.; Shung, A. K.; Jo, S.; Mikos, G. *Biomacromolecules* **2002**, *3*, 153−158.
(21) Bhattarai, N.; Ramay, H. R.; Gunn, J.; Matsen, F. A.; Zhang, M. *J. Controlled Release* **2005**, *103*, 609−624.
(22) Yu, L.; Zhang, H.; Ding, J. A. *Angew. Chem., Int. Ed.* **2006**, *45*, 2232−2235.
(23) Jo, S.; Kim, J.; Kim, S. W. *Macromol. Biosci.* **2006**, *6*, 923−928.
(24) Kim, M. S.; Hyun, H.; Khang, G.; Lee, H. B. *Macromolecules* **2006**, *39*, 3099−3102.
(25) Coulembier, O.; Mespouille, L.; Hedrick, J. L.; Waymouth, R. M.; Dubois, P. *Macromolecules* **2006**, *39*, 4001−4008.
(26) Wang, H.; Hua, J.; Qui, K. Y. *J. Polym. Sci., Polym. Chem.* **1998**, *36*, 695−702.
(27) Zhang, Y.; Zhou, R. X. *Biomaterials* **2004**, *26*, 2089−2094.
(28) Sangeetha, N. M.; Bhat, S.; Choudhury, A. R.; Maitra, U.; Terech, P. *J. Phys. Chem. B* **2004**, *108*, 16056−16063.
(29) Li, H.; Yu, G.-E.; Price, C.; Booth, C.; Fairclough, J. P. A.; Ryan, A. J.; Mortensen, K. *Langmuir* **2003**, *19*, 1075−1081.
(30) Bae, S. J.; Joo, M. K.; Jeong, Y.; Kim, S. W.; Lee, W. K.; Sohn, Y. S.; Jeong, B. *Macromolecules* **2006**, *39*, 4873−4879.
(31) Li, X.; Liu, W.; Ye, G.; Zhang, B.; Zhu, D.; Yao, K.; Liu, Z.; Sheng, X. *Biomaterials* **2005**, *26*, 7002−7011.
(32) Arotcarena, M.; Heise, B.; Ishaya, S.; Lascheesky, A. *J. Am. Chem. Soc.* **2002**, *124*, 3787−3793.
(33) Brand, L.; Seliskar, J.; Turner, D. C. The effect of chemical environment on fluorescent probes. In *Probes of Structure and Function of Macromolecules and Membranes*; Chance, B., Lee, C. P., Blaisie, J. K., Eds.; Academic Press: New York, 1971; pp 17−39.
(34) Wang, H.; Hua, J.; Qui, K. Y. *J. Polym. Sci., Polym. Chem.* **1998**, *36*, 695−702.
(35) Zhang, Y.; Zhou, R. X. *Biomaterials* **2004**, *26*, 2089−2094.
(36) Chung, Y. M.; Simmons, K.; Gutowska, A.; Jeong, B. *Biomacromolecules* **2002**, *3*, 511−516.
(37) Verduin, H.; de Gans, B. J. Dhont, J. K. G. *Langmuir* **1996**, *12*, 2947−2955.
(38) Jun, Y. J.; Toti, U.S.; Kim, H. Y.; Yu, J. Y.; Jeong, B.; Jun, M. J.; Sohn, Y. S. *Angew. Chem., Int. Ed.* **2006**, *45*, 6173−6176.
(39) Jeong, B.; Windisch, C. F., Jr.; Park, M. J.; Sohn, Y. S.; Gutowska, A.; Char, K. *J. Phys. Chem. B* **2003**, *107*, 10032−10039.
(40) Tu, R. S.; Tirrell, M. *Adv. Drug Delivery Rev.* **2004**, *56*, 1537−1563.
(41) Lee, H. J.; Yang, S. R.; An, E. J.; Kim, J. D. *Macromolecules* **2006**, *39*, 4938−4940.
(42) Jeong, B.; Bae, Y. H.; Kim, S. W. *Colloids Surf., B* **1999**, *16*, 185−193.
(43) Zupancich, J. A.; Bates, F. S.; Hillmyer, M. A. *Macromolecules* **2006**, *39*, 4286−4288.
(44) Dobrynin, A. V.; Rubinstein, M. *Macromolecules* **2000**, *33*, 8097−8105.
(45) Jeong, B.; Bae, Y. H.; Kim, S. W. *J. Biomed. Mater. Res.* **2000**, *50*, 171−177.

MA070190Z